Journal Pre-proof

Design, Optimization, and Characterization of Zolmitriptan Loaded Liposomal Gels for Intranasal delivery for acute migraine therapy

Chettupalli A.K., Sunand Katta, Mohd Vaseem Fateh, M. Akiful Haque, Daniel Kothapally, Dr Prasanth Damarasingu, Budumuru Padmasri, Palavalasa. Archana

PII: S2949-866X(24)00074-1

DOI: https://doi.org/10.1016/j.ipha.2024.07.003

Reference: IPHA 130

To appear in: *Intelligent Pharmacy*

Received Date: 19 June 2024

Revised Date: 3 July 2024

Accepted Date: 7 July 2024

Please cite this article as: Chettupalli AK, Katta S, Fateh MV, Haque MA, Kothapally D, Damarasingu DP, Padmasri B, Archana P, Design, Optimization, and Characterization of Zolmitriptan Loaded Liposomal Gels for Intranasal delivery for acute migraine therapy, *Intelligent Pharmacy*, https://doi.org/10.1016/j.ipha.2024.07.003.

Design, Optimization, and Characterization of Zolmitriptan Loaded Liposomal Gels for Intranasal delivery for acute migraine therapy

Chettupalli A.K.[1*], Sunand Katta[2], Mohd Vaseem Fateh[3], M. Akiful Haque[4], Daniel Kothapally[5], Dr Prasanth Damarasingu[6], Budumuru Padmasri[7], Palavalasa. Archana[8]**

[*1]Department of Pharmaceutical Siences, School of Pharmacy, Galgotias University, Greater Noida, Uttar Pradesh -203201, India. ananda.chettupalli@galgotiasuniversity.edu.in

[2]Centre for Nanomedicine, Department of Pharmaceutics, Anurag Group of Institutions, Venkatapur, Ghatkesar, Medchal, Hyderabad -500088, Telangana, India.

[**3]School of Pharmacy and Research Centre, Sanskriti University, Mathura 281001, Uttar Pradesh, India;

[4]School of Pharmacy, Anurag University, Venkatapur (V), Ghatkesar (M), Medchal Malkajgiri, Telangana-500088, India;

[5]Department of Pharmaceutics, Chaitanya Deemed to be University, Kishanpura, Hanamkonda, Warangal-506001, Telangana.

[6]Department of Pharmacology, School of Pharmacy, Centurian University of Technology and Management, Gopalpur, Balasore-756044. .

[7]Department of Pharmaceutical technology, Sri Venkateswara College of Pharmacy, Etcherla, Srikakulam, Andhra Pradesh-532410.

[8]Sri Venkateswara college of pharmacy, Etcherla- 532410, Srikakulam, Andhra Pradesh.

Corresponding author emails: ananda.chettupalli@galgotiasuniversity.edu.in **;**
mohammad.vaseem55@yahoo.com **

Abstract

Zolmitriptan is the primary drug for the treatment of Migraine. However, the bioavailability of the drug is low and requires repetitive administration leading to side effects. Zolmitriptan's bioavailability can be improved by incorporating it into liposomes as a topical intranasal gel. The formulation was developed using a Central composite design employing a response surface approach. The new formulations were tested for particle size, shape, drug entrapment efficiency, and in vitro drug release. Permeation experiments and histopathology in rats were also conducted to determine the formulation's safety. The vesicle size was found to be in the range of 103.82±7.16 to 694.38±1.02 nm, zeta potential --19.28 to -32.8 mV, Entrapment Efficiency from 55.49±1.37 to

99.12±0.36 %, and cumulative drug release from 59.71±6.94 to 99.38±0.13 % respectively. In-vitro drug release of G1 and G3 gel formulations showed a non-Fickian released pattern during the studies. A comparison of the permeation coefficient of G1 (0.539 µg/cm2) and G3 (5.3 µg/cm2) showed a slight variation in the drug release rate after 24 hrs. For the liposomal gel and its solution, we found a significant difference in drug penetration of p0.05 after 12 hours compared to the control gel. There were substantial differences in bioavailability and pharmacokinetics between the optimal Liposomal Gel Formulation and other formulations, including the drug solution, liposomal suspension, and optimized formulation F12. The liposomal gel is non-irritating and safe for topical administration by histopathological investigations. Therefore, the study demonstrated that Zolmitriptan Liposomal gel has better efficacy, good tolerability, and enhanced bioavailability, making it an optimal treatment for acute Migraine.

Keywords: Zolmitriptan; Cholesterol; Liposomal gel; Central composite design; Soya lecithin; Pharmacokinetics; skin permeation, micelles formation.

Introduction

One of the world's most debilitating medical conditions is Migraine, a chronic neurological ailment affecting millions worldwide. Most of the population is impacted, but women are four times more affected than males during their most productive years of employment [1]. Scientifically, migraines are characterized by constant attacks of headaches and different symptoms linked to the autonomic nervous system. Migraine attacks the AURA (initial visual disturbances) followed by scintillating scotoma leading to a unilateral or bilateral throbbing headache, repeatedly accompanied by photophobia, vomiting, nausea, and finally collapse. Historically, Methysergide was the first drug of choice for treating Migraine [2].

Efforts made by the experts to develop nano-particulate carriers have led to the formulation of micelles, dendrimers, liposomes, nano-suspensions, and emulsions. Drugs integrated into nanocarriers are clinically used for many diseases. Oral, nasal, pulmonary, and parenteral modes of administration are all successful with this drug delivery system [3]. Earlier studies have shown that Zolmitriptan (ZMT) repeated therapy had no meaningful effect and failed to provide safety and effectiveness [4,5]. There is a limited duration to the drug's pain-relieving effect because of its quick breakdown.

The study mainly emphasizes developing a liposomal gel formulation (LGF) of ZMT for enhanced action against Migraine. The nasal route of administration is gaining importance with alternative methodologies like the novel peptides [8,9]. The advantage of the nasal route is its high vascularity in the epithelium layer, which can avoid drugs' first-pass metabolism, thereby enhancing their efficacy [10]. Novel drug delivery systems have become a breakthrough in the current research era and aim to release drugs in a controlled manner with no or minimal side effects. The medication is delivered to the site of action via various carriers or vehicles, and the concentration of the drug in the blood is maintained [4]. The cells in lipid layers have a variety of applications in the fields like immunology, genetic engineering, and diagnostics in membrane biology [10,11]. Vesicles offer a choice of modifying the membranes, facilitating therapeutic action at a given site.

The convenience of nasal drug delivery allows a fast administration with better patient compliance and reduced product cross-contamination. ZMT, as LGF, could denote an alternative to available oral administration for enhanced bioavailability and efficacy. Despite its efficacy as a nasal drug delivery system, some limitations must be addressed. The irritations caused in the tissues by formulation components and degradation are the leading causes of concern. However, the mucociliary clearance time can decrease the residing period of drugs in the olfactory region [12].

ZMT is a potential 5-hydroxytryptamine 1B, 1D-receptor agonist recommended as an anti-migraine agent. ZMT has approximately 40 % bioavailability and t1/2 of 3 hours. The available ZMT marketed preparations are 2.5 mg dosage in the form of buccal tablets and 5 mg as nasal sprays. The present study mainly emphasizes developing an optimal ZMT as an LGF using a response surface methodology (Central Composite Design). The cumulative drug release (% CDR) must be rapid and effective to achieve the pharmacological effect. Mild to severe headaches respond well to ZMT, a water-soluble, fast-acting medication. The use of ZMT-loaded liposomes in the treatment of acute Migraine represents a significant development. This research aimed to create an intranasal formulation for acute Migraine that would have a higher bioavailability and be more targeted since it was administered through the nasal passages. As part of this study, the gelling characteristics of several polymers (e.g., Carbopol-934, Poloxamer-407, hydroxyl propyl methyl cellulose-K100) were evaluated in relation to the nasal cavity. The gel strength and mucoadhesive characteristics of the improved formulations were examined further.

Materials and methods:

Dr. Reddy's Labs in Hyderabad, India, donated ZMT and API, while S.D. Fine-Chemicals Pvt. Ltd. in Mumbai, India, provided Cholesterol and Soya lecithin. Merck laboratory in Mumbai, India, supplied the chloroform. Fisher Scientific in Mumbai, India, provided the triethanolamine. The Research lab fine chem. Industries in Mumbai, India, provided the Span-60. Sample Carbopol-934 was given to hetero labs by hetero laboratories in the Indian city of Hyderabad.

Animal source

We purchased the experimental animals from the National Institute of Nutrition, Telangana, India. Injectable agent Thiopental sodium of 30 mg/kg was used by IV to produce euthanasia in experimental animals.

Experimental Design

Preparation of Liposomes

CCD was used to prepare ZMT -loaded liposomes, and results were derived using the linear regression method [10]. Elastic Liposomes have better skin penetration due to their more extraordinary deformable nature than ordinary liposomes. The liposomal suspension was developed by the conventional rotary melting sonication method. Liposomes were made in batches with various quantities of Cholesterol and soya lecithin as excipients. The loaded bulk of Cholesterol, soya lecithin, and drug were appropriated in an orderly manner with an equal proportion of chloroform-triethanolamine (1:1) mixture [27]. Excess solvent was evaporated using a rotary evaporator at 130 rpm and 40°C. We used an orbital shaker at 60 revolutions per minute to hydrate the collected lipid layer with a (7 percent v/v) ethanol solution for roughly an hour. Consequently, the vesicles we generated were inflated for two hours at 24 oC to produce enormous multilamellar ones. A probe sonicator (UP50H, Hielscher Ultrasonics) at 50 W for 10 minutes was used to create small vesicles [28].

For the formulation of ZMT liposomes, the soya lecithin, Cholesterol, and span-60 concentrations were treated as independent variables. The % EE, Vesicle size, and % CDR were dependent variables.

Experimental design for the formulation of liposomes

The ease with which a statistical design such as CCD can be implemented and interpreted while requiring fewer experimental runs than other methods make it the widely accepted method for developing a response surface methodology (RSM) [29].

Evaluation of Liposomes

ZMT -loaded liposomes were evaluated for drug entrapment using an Ultra-micro centrifuge at 3000 rpm at 4oC for 45 min. Using a 283nm UV-visible spectrophotometer, ZMT was calculated (UV 3200, Lab India.). Analysis of liposome properties such as the Zeta potential (ZP) and Poly-dispersibility index (PDI) was carried out utilizing a zeta-sizer (Malvern-3000, Zeta sizer, Malvern, India). Liposomes were confirmed using a trinocular microscope at 40x magnification, and the formulations were analyzed by Scanning Electron Microscopy (S-3700N, Hitachi, Japan) and Transmission Electron Microscopy (JEOL-JEM2100-200KV, USA)[30]

Determination of Gelation Temperature

The gelation temperature of Poloxamer-188 (10 percent w/v) dissolved in water was obtained using a visual examination approach [31]. The temperature was maintained at 1 oC/min by keeping 10 ml of Poloxamer-188 in a digital magnetic stirrer. The gelation temperature measures the temperature at which a gel forms.

It was determined by taking 5 mL of each formulation and swirling it with a magnetic stirrer in 20 mL of water. It was necessary to put a thermometer into the formulation to keep an eye on the heat flow at a rate of one degree Celsius per minute at 30 revolutions per minute. Recordings were made of the gelation temperature and duration on each bar. The data were presented as the mean and standard deviation (n=3).

Preparation of in-situ ZMT liposomal nasal gel formulation

The proposed formulation was prepared by dispersing different quantities of HPMC-K100 and Carbopol-934 as mucoadhesive agents. Poloxamer-188 solutions were added (Table 1) and continuously stirred until gel was formed. For further evaluation, this was stored at room temperature [32].

Table 1. Composition of ZMT -loaded LGF.

S. No	Formulation code	Drug (mg)	Poloxamer 188 (%w/v)	Carbopol 934	HPMC K100
1	ZMT	10	-	-	-
2	ZMT	10	14	-	-
3	G1	10	14	0.5	-

4	G2	10	14	1.0	-
5	G3	10	14	1.5	-
6	G4	10	14	-	0.5
7	G5	10	14	-	1.0
8	G6	10	14	-	1.5
9	G7	10	14	1.0	1.0

Evaluation of in-situ gel formulation

We tested the liposomal gels for clarity, pH, percent drug load, and viscosity utilizing critical criteria. We employed a clarity test gadget to make sure everything was crystal clear. The pH was determined using a pH meter (PICO+ pH Meter, Lab India, India). The % drug content was determined using a UV-Visible spectrophotometer (UV-1800, Shimadzu, Japan) at 283 nm. Viscosity was measured using a Brookfield viscometer (LVDVE, Brookfield, U.S.A.) [33].

Vesicle size and Size distribution

The ZMT liposome vesicle size was determined by optical microscopy using a point eyepiece micrometer. A total of 100 molecules per batch were calculated for their amount. After sonication, we found the vesicle size using a particle size analyzer [34].

% EE

In a test tube with a fissure size of 20 mm, 0.5 ml of dispersion concentrate was appropriated. The open end of the tubes was sealed with a semi-permeable dialysis membrane. These were inverted and clamped with support over the surface of 100 mL water in a 250 mL beaker, slightly below the water surface. To avoid a whirlpool, a magnetic stirrer was utilized. For subsequent examination, we kept the samples at 37° C. The % CDR of liposomes passed through the membranes and into the receptors chamber medium. A UV-visible spectrophotometer measured the absorbance at 283 nm of 2 ml of sample filtrate taken from the receptor chamber media. The sample was then replenished with 2 ml of new buffer medium [35]. The % EE in the gel was determined using the equation below.

$$\% \text{ EE } = \frac{\text{Amount of Drug Encapsulated}}{\text{The total amount of drug used in the formulation}} X\ 100$$

Drug compatibility studies

FT-IR

Excipients, their mixtures, and drug incorporated in ZMT -loaded LGF were blended, each separately, with IR grade potassium bromide in a ratio of 1:100 to form discs in a hydraulic press at 15000 psi pressure and were observed using an IR spectrophotometer (Hitachi 295, Japan) at the wavelength of 4000-400 cm^{-1} [36].

DSC

Drug/excipient interactions/polymorphism were investigated using DSC to determine the thermotropic characteristics and interrelationships. At a flow rate of 100 ml/min of nitrogen, the aluminum pan containing 5 mg of sample was heated to between 40 and 300 ºC for 10 minutes at a rate of 10 ºC/min [37].

XRD

The crystalline state of the formulation was determined using an X-ray diffractometer with a copper target at a current and voltage of 20 mA and 40 kV, respectively [37]. The scanning rate was maintained at 0.30 ºC/min.

Microscopic examination

The formulated gel was spread as a thin layer on a microscopic slide and observed for liposomal cell structure and any insoluble crystals using a light microscope under the magnification power of 40x [22].

SEM

Diluted with distilled water, the ZMT-loaded LGF was adsorbed onto a film-coated copper grid and air-dried before being analyzed. Gold or palladium was vacuum-coated onto this after it was dyed with a 2 percent phosphor-tungstic acid solution. SEM at a voltage of 15 kV was used to obtain the surface pictures [38].

TEM

It was determined that ZMT-loaded LGF has distinct morphological characteristics. Adsorption of the diluted LGF onto a carbon-coated copper grid for TEM evaluation took place after a 10-minute drying period at room temperature [38].

Skin Irritation Test

Institutional Animal Ethics Committee (Ref. No. I/IAEC/NCP/009/2020R or) approved animal research conducted in Nalgonda, Telangana, India, under the Committee for Control and Supervision of Experiments on Animals. Three sections of skin were removed after shaving the rat's belly hair. We placed a one-inch glass ring over the abdomen's skin. Liposomes containing ZMT, 0.5 percent paraformaldehyde, and aqueous water (the control group) (positive control group). 0.5 ml of the solution was placed in a glass ring and allowed to sit for 24 hours [39]. For 24 hours, the skin of the exposed drug solution was excised and stored in a formaldehyde solution with a concentration of 5 percent. Horizontal section incisions were made, and paraffin wax was applied to the exposed skin. Stains of eosin and hematoxylin were applied sequentially to the sections. ZMT - LGF was rated on a scale of 0-none, 1-slight, 2-well defined, 3-moderate, and 4-severe for edema when applied to the skin, based on the study's results. Edema and erythema were assessed using the erythematic scale of 0-none, 1- to 2-mild, 3-moderate, and 4-scar formation. The following is the formula used to arrive at the preceding two results: From 0 to 1, mild irritation, 3 to 5, moderate irritation, and severe pain are all represented by a number between 0 and 8.

In-Vitro Diffusion Studies: % CDR from the semi-permeable membrane

ZMT-liposomal gel's in-vitro percent CDR was determined using the Franz diffusion cell. The semi-permeable membrane was treated with LGF, and the receptor chamber was filled with phosphate buffer (pH 7.4), which was agitated at 500 rpm and maintained at 37 °C. The drug content of 5 ml samples obtained at regular intervals was tested using a UV-visible spectrophotometer set at 283 nm (replacing the same amount with buffer).

Ex-Vivo Permeation Studies

In a laboratory setting, a group of 180-200 g male Wistar rats was fed and watered ad libitum. Thiopental sodium (30 mg/kg) was used to execute the rats. Vertical Franz diffusion cells were used to examine the excised porcine nasal mucosa. It took two hours to clean and store the nasal cavity's whole mucosal membrane in the buffer. Franz diffusion cells were linked to this. At a steady speed and temperature, 2.5 mg of ZMT-liposome gel was placed into the donor compartment, and phosphate buffer (pH 5.5) was added to the receptor compartment. 7 mL of pH 7.4 phosphate buffer was added and stirred with a magnetic stirrer at 50 pm while the receiver medium was kept at 37 °C. It was done systematically, with the same amount of medium being replenished for each 0.5 ml sample obtained at regular intervals (e.g., 15 minutes, 30 minutes, 1 h,

2 h, 3 h). A UV-visible spectrophotometer was then used to examine the samples, and the permeability coefficient was calculated as follows: (P). The comparative research used Carbopol-934, a liposomal gel, and a controlled solution.

Permeability coefficient (P) = dc/dt x V/ AC

In vivo study

The rabbits' abdomens were shaved and thoroughly cleaned two hours before treatment. Drug analysis was made simpler by inserting an adapter into the right femoral artery. ZMT levels in rabbit plasma were determined by HPLC utilizing ZMT-Liposomes and ZMT-Liposomal gels obtained from the plasma of rabbits. The ZMT formulation was quantified using a Shimadzu LC–10AT HPLC system with LC10 software and an SPD–10A UV/Vis detector. At a temperature of 23 °C, a 150 3.9 mm ID Symmetry C18 column with a particle size of 4 m was used to separate the samples. With a constant flow rate of 1.5 mL/min, a 30:30:40 mixture of water, methanol, and acetonitrile served as the mobile phase in the assay. A wavelength of 254 nm was used for detection. Ortho-phosphoric acid was used to modify the pH of the mobile phase to 2.5. The rheodyne injection port received 20 µl of each sample. ZMT had a retention time of 3.8 minutes. We looked at the outgoing effluent using a 254 nm wavelength. HPLC determined ZMT plasma concentrations after blood samples were drawn from the femoral artery and stored in heparinized tubes for 24 hours.

Heparinized glass tubes containing 4.0 ml of blood were placed in the patient's femoral artery and spun at 4000 RPM for 10 minutes to extract 2 ml of plasma, frozen until testing. Blood samples were taken at intervals of 0.15, 0.30, 0.45, 1, 2, 3, 4, 8, 12, 16, 18, 22 and 24 hours after transdermal administration. After collecting blood samples, injecting heparinized physiological saline (75 I.U./ml) into the rabbits' ear veins kept their homeostasis intact.

Pharmacokinetic data analysis

Mean plasma drug concentration (SD) was shown over time for six rabbits. To calculate various parameters, such as the maximum plasma concentration (C_{max}), the time to reach C_{max} (T_{max}), the mean residence time from zero to infinity (MRT(0–), h), and the mean residence time from zero to the last sampling point AUC(0–t)(h), the area under the curve from zero to the last sampling point AUC(0–t) (ng. h/mL), and the elimination half-life ($T_{1/2}$, h), this plot was used to calculate various parameters, such as the maximum plasma concentration (C_{max}), the time to reach C_{max} (T_{max}, h), and the mean residence time from zero to time t (MRT(t)(h), the elimination.

Histopathology

On the dorsal side of the rat's skin, LGF and a hydroalcoholic mixture of drugs were applied for 24 hours and fixed on the diffusion cell. Gels were wiped off from the skin, and then the skin tissues were fixed in formalin-saline solution (10 % v/v) for about 72 hrs. Vertical sections were stained and examined under a microscope. These studies reveal the mechanism of penetration enhancing the ability of liposomes and the compatibility of liposomal vesicles with the skin.

Docking studies

ZMT, Soya Lecithin, and Cholesterol were obtained from the National Library of Medicine-PubChem (https://pubchem.ncbi.nlm.nih.gov/). Using the polymers Soya Lecithin and Cholesterol, we used ChemDraw Ultra 8.0 to build the circular micelle, which was then converted to mol file format using the program. Using the Convert-UNM Bio-computing-The University of New Mexico, ChemDraw may be converted to a mol file format if there are more than 999 atoms or bonds in the molecule. The micelle's mol file to PDB format by BIOVIA Discovery Studio Visualizer. The PDB file was loaded into PyRx Virtual Screening Tool [42] and transformed to a pdb qt macromolecule. A universal force field [43] was used to decrease the energy of the ligand. The ZMT was then exposed to molecular docking, first with Soya Lecithin and subsequently with micelle, as described by Khan et al. [44]. The three-dimensional grid box was designed to cover the whole docking target structure. Figure 1 shows the structures of ZMT, Soya Lecithin, and Cholesterol.

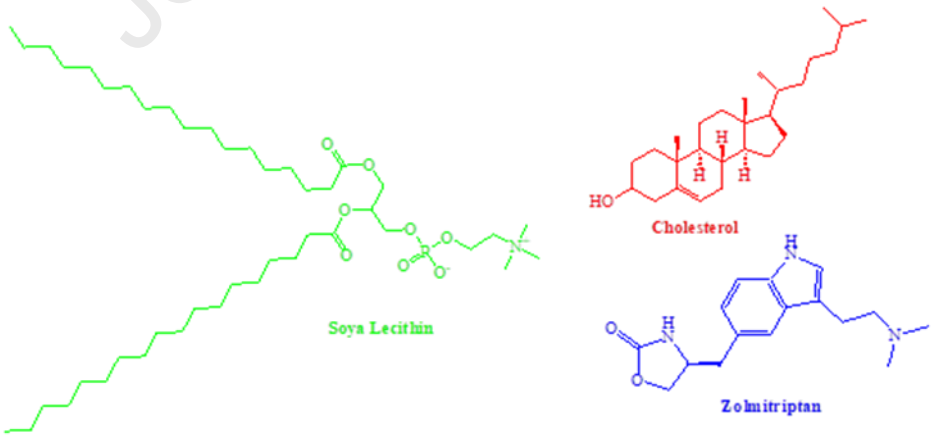

Figure 1. The structures of ZMT, Soya Lecithin, and Cholesterol.

The use of molecular docking generated a total of nine conformers. Root mean square deviation/upper bound (RMSD/up) and root mean square deviation/lower limit (RMSD/lb) were the best models. Figure 2 displays a micelle of soya lecithin and Cholesterol.

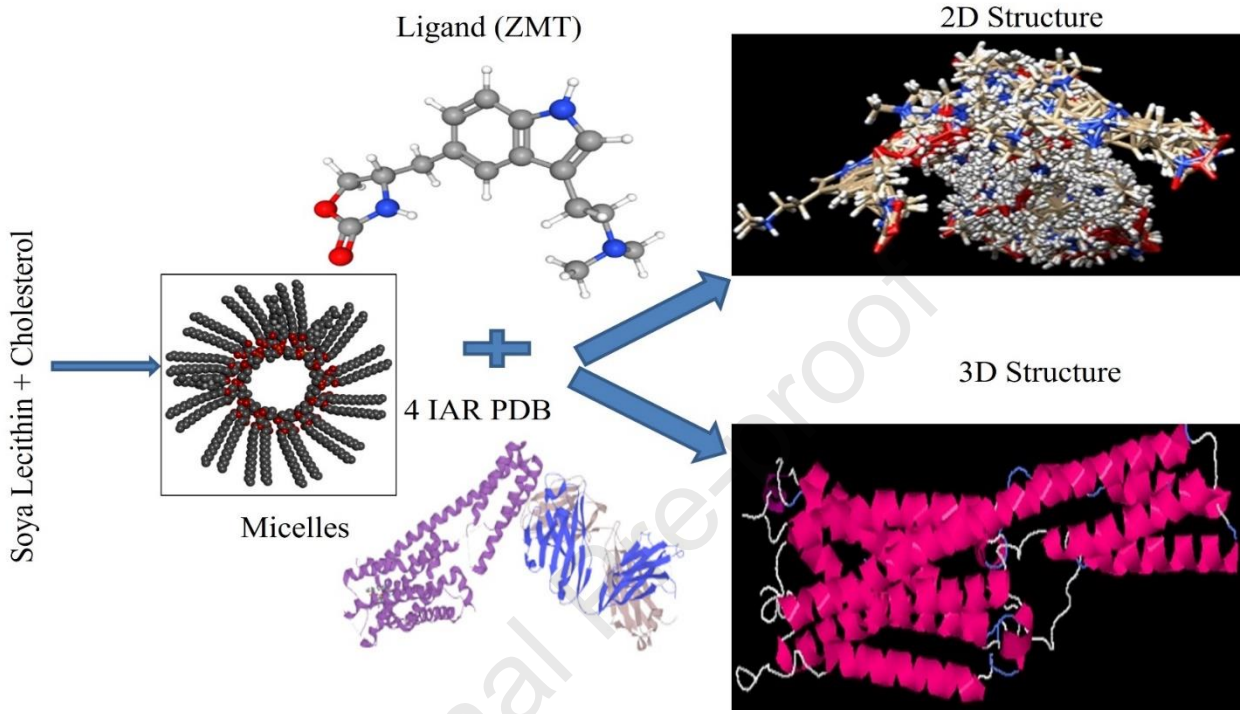

Figure 2. A designed micelle of soya lecithin and Cholesterol, docking formation in 2D & 3D

Results and Discussion

Preparation of liposomes

Cholesterol (X1), soya lecithin (X2), and Span 60 (X3) were shown to have a significant effect on the dependent variables of percent Entrapment Efficiency (Y1), particle size (Y2), and percent Cumulative Drug Release (Y3) using the Central Composite Design (CCD) (Table 2). We used Design-Expert software version 12.0.3.0 to develop binominal equations.

Table 2. Dependent and independent values of different parameters of ZMT-loaded liposomal formulation.

Independent Variables			
Parameter	**Low (-1)**	**Medium (0)**	High (+1)

X1 (mg)	200	300	400
X2 (mg)	100	350	600
X3 (ml)	0.5	1.5	3
Dependent variables			
Y1 (%)	55.49±1.37		99.12±0.36
Y2 (nm)	103.82±7.16		694.38±1.02
Y3 (%)	59.71±6.94		99.38±0.13

X1, concentration of Cholesterol; X2, concentration of Soya lecithin; X3, concentration of Span 60; Y1, % EE; Y2, Vesicle size; Y3, % CDR

Formulation and optimization of Liposomes containing ZMT

For the liposomes containing ZMT, we used the conventional rotary melting sonication method [13,14]. This approach is most often used to manufacture elastic liposomes. Data analysis and formulation optimization using Design-Expert® software were carried out. [15]. This study's independent and dependent variables were Cholesterol (X1), lipid (X2), and Span 60 (X3), respectively. Based on our comprehensive literature search and early experiments [28], we arrived at our list of independent variables and their corresponding levels. Following the CCD, twenty formulations were made, and the results are reported in Table 3 for percent CDR, the size of the vesicles, and EE. Linear regression, two-factor interaction (2FI), and quadratic models were some of the mathematical models used to match the data. A second-order polynomial equation with interaction and quadratic components was derived by fitting the observed responses to a multiple linear regression model. The following is an example of the generic form of a polynomial equation:

$$Y = \beta o + \beta 1Z1 + \beta 2Z2 + \beta 3Z3 + \beta\ 12\ Z1Z2 + \beta\ 23Z2Z3 + \beta\ 13Z1Z3 + \beta\ 11Z1\ 2 + \beta\ 22Z22 + \alpha 33Z32 \quad (1)$$

This model has three dependent variables, Y (1–3), arithmetic mean response of 0, linear coefficients of 1, 2, 3, and interaction coefficients of +123, as well as independent variables X (1–

3) with coded levels of 11, 22, and 33. X1 denotes interaction and quadratic terms through X3 in the last step of the equation.

After taking into account the magnitudes of the coefficients and the mathematical signs of those coefficients, a decision was made using the polynomial equation. It is possible to identify statistically significant words with higher coefficient values and non-statistically significant phrases with lower coefficient values. Increasing one variable causes this reaction to rising, while increasing the other variable causes this reaction to decrease, according to the polynomial equation. The statistical significance of the model and model terms was investigated using ANOVA. As long as the probability value for any model or model term is p 0.05, it is considered significant. Constructing 3D response surfaces and perturbation graphs with De-sign-Expert® helped us better grasp the relationship between independent and dependent variables. The model's validity was tested using linear correlation graphs of anticipated and actual values. R2 >0.90 for all responses [30] indicates a good match between expected and actual values. DoE program selected the optimum formulation based on point prediction. A quadratic model was used to optimize the formulation parameters.

Table 3. Observed response from CCD of ZMT-loaded Liposomal formulations.

Formulation	F1	F2	F3	Y1	Y2	Y3	Zeta (-mV)	PDI
F1	+1	+1	+1	55.87±1.27	650.46±3.56	59.79±2.31	-27.56	0.351
F2	0	0	0	98.24±0.51	112.49±5.46	97.35±0.59	-25.34	0.315
F3	+1	-1	-1	78.53±2.11	420.28±2.89	78.61±4.16	-29.37	0.259
F4	0	0	0.352	65.12±2.51	411.34±6.12	82.28±2.23	-23.37	0.319
F5	-1	+1	-1	55.49±1.37	429.17±5.16	69.79±7.16	-27.53	0.297
F6	0	0	3.852	78.81±2.01	320.29±4.29	78.94±1.58	-25.29	0.302
F7	-1	-1	+1	68.94±0.59	300.29±7.05	73.68±2.13	-29.17	0.271
F8	0	0	0	99.12±0.36	300.59±5.46	98.59±0.64	-22.56	0.328

F9	-1	+1	+1	87.59±2.38	112.46±9.01	87.62±3.12	-19.28	0.361
F10	-1	-1	-1	65.37±1.39	436.73±8.72	62.97±2.16	-24.81	0.291
F11	0	0	0	97.14±1.12	264.91±6.14	99.38±0.13	-30.28	0.315
F12	**0**	**0**	**0**	**98.26±1.06**	**103.82±7.16**	**99.38±0.16**	**-32.8**	**0.251**
F13	0	0	0	94.78±2.1	109.37±4.16	98.67±1.10	-28.34	0.284
F14	0	0	0	97.16±0.46	104.46±7.18	98.67±1.23	-26.17	0.259
F15	0	770.4	0	67.26±2.29	560.53±3.12	69.83±6.01	-26.84	0.326
F16	131.8	0	0	76.48±2.43	285.43±7.46	77.73±4.53	-29.74	0.368
F17	0	-70.44	0	79.35±3.10	385.74±3.12	70.64±3.87	-28.92	0.413
F18	+1	+1	-1	55.96±2.89	694.38±1.02	59.71±6.94	-26.51	0.426
F19	468.17	0	0	58.92±3.11	571.38±0.13	59.89±5.89	-29.17	0.451
F20	+1	-1	+1`	56.37±2.13	384.94±3.64	60.79±5.46	-27.13	0.398

Optimization of ZMT-Liposomes based on Central Composite Statistical Design

The CCD is thought to effectively determine the factors' individual and mutual effects on the desired results. In addition, CCD is more efficient and less risky than other systems. Analysis of variance (ANOVA) was performed to examine the relationship between the chosen response variables (Y1-Y3) and the independent variables (X1-X3). The Central Composite design was utilized to identify the elements that have a tangible impact on the selected response variables. CCD design was used to make twenty trial batches, and the results were compiled in F12. ANOVA was used to analyze the data using Design Expert® software. Many models were tested, but only one had an F-value of more than 1. 3D response surface frames were used to examine the interplay between two different impacts on a single response (Figure 1).

The statistical significance of the model is shown by its F-value of 56.14. Noise has a 0.01% probability of causing an F-value of this magnitude. Significant model terms have P-values

less than 0.05. It is important to note that A2, B2, and C2 are model terms that are relevant in the present circumstance. For larger values, the model terms are not relevant. There is a significant lack of fit, as shown by the F-value of 7.84. There is only a 2.06% chance of a substantial Lack of Fit F-value occurring due to noise.

The Predicted R2 of 0.865 and the Adjusted R2 of 0.963 are within 0.2 of each other. Adeq. The signal-to-noise ratio is a measure of precision. More than a four-to-one ratio is preferred. 19.259 indicates a strong signal, according to the signal-to-noise ratio. Using this approach, you may find your way around the creative environment.

$$Y1=97.57 - 4.40X1 - 2.53X2 + 2.66X3 - 3.98X1X2 - 7.24X1X3 + 6.32X2X3\ 11.33X1^2 + 9.35X2^2 - 9.82X3^2 \quad (1)$$

Many studies showed that improving the quantity of soya lecithin and span-60 ultimately improves % EE (Figure 3). ZMT is soluble in soya lecithin due to its lipophilicity, the prime determinant for enhancing EE. Span-60 plays a synergistic role that further enhances % EE of the multilamellar liposomal vesicles [17].

The Model F-value of 65.94 suggests that the results are statistically significant. F-values greater than 0.01% can only exist owing to random noise. P-values of less than 0.0500 are considered significant. This circumstance necessitates using A, B, AB, A2, B2, and C2. If the value is higher than tenths of a percent, the model terms are of little consequence. If the model has many insignificant terms, model reduction may improve it. The lack of fit is significant, as shown by the high F-value of 102.43. Only 0.01% of the time will a substantial Lack of Fit F-value arise because of noise. In this case, the Adjusted R2 of 0.968 is within 0.2 of the Predicted R2 of 0.875, so the difference is less than 0.2. There should be a ratio of at least four. At 23.918 dB, the intensity of your signal is adequate. Using this approach, you may find your way around the creative environment.

Liposomal vesicle size is directly and indirectly linked to the amount of ethanol and Cholesterol utilized in the formulation. Alcohol and Cholesterol may produce a negative charge on the liposomal surface, which reduces the size of the vesicle and helps stabilize the dispersed particles by steric stabilization. Lipid solubilization is accelerated by the presence of both ethanol and surfactants at high concentrations. Because the soy lecithin concentration is directly

proportional to the size of the vesicle, the binominal equation suggests that the molecules of soy lecithin consolidate, increasing the vesicle's size and instability [18].

Statistics show that the model has a substantial F-value of 80.62. Here, key model terms like A2, B2, and C2 come into play. There is a significant lack of fit based on the F-value of 20.56. A considerable deficiency in Fit F-value has a 0.24 percent chance of being caused by noise. With an Adjusted R2 of 0.974, the model's predicted R2 of 0.895 is slightly off by 0.2. Measures the signal-to-noise ratio, or S/N ratio. There should be a ratio of at least four. At 23.656 dBm, the signal strength is sufficient.

$$Y3=8.7558 - 4.77146X1 - 0.0367766X2 - 0.379503X3 - 5.0825X1X2 - 5.785X1X3 + 3.1275X2X3 - 11.0973X1^2 - 10.5935X2^2 - 6.92536X3^2 \quad (2)$$

The percentages of CDR with X2 and X3 variables are shown with + and – marks, respectively. Stat-Ease software was used for statistical analysis, and the significance criteria were p 0.05 for ANOVA (Tables 2 and 3). As a result of surface response curves and contour plots, it can be concluded that the optimized formulation has superior properties (percent EE, Vesicle Size, percent CDR) than the unoptimized formulation (Figure. 2). Although the model had an F-value of 0.497, the noise had an F-value of 0.503. This F-value had a 32.03 percent probability of occurring due to noise. We didn't need to reduce our model since the model terms with P 0.05 were significant. The data presented shows a solid relationship between the F-value for Lack of Fit and the total error. This figure has a 45.35 percent probability of occurring due to noise.

After gathering responses for all formulation batches, we used numerical optimization to optimize the process parameters simultaneously, resulting in ZMT-Liposomes with the required dependent responses. The Design Expert® program required us to apply restrictions to all three process parameters to achieve a formula for ZMT -Liposomes with the smallest Vesicle size, highest % EE, and highest CDR. Because the optimized batch matched the independent variables' anticipated values, as shown in Table 3, this confirms the Central Composite Design's predictability. The ZMT Liposomes optimized batch had a desirability score of 0.889, the highest possible score. Low percentage bias between anticipated and experimental response data proved the CCD's statistical validity. "Cholesterol and phospholipids were combined in a liposomal composition as a control to compare the fundamental difference between liposomes and elastic liposomes (Figure 3). Studies involving high temperatures and drug retention showed that the medication was leaking

out of the body. Lipid bilayers may become more fluid at higher temperatures, leading to membrane packing problems [16].

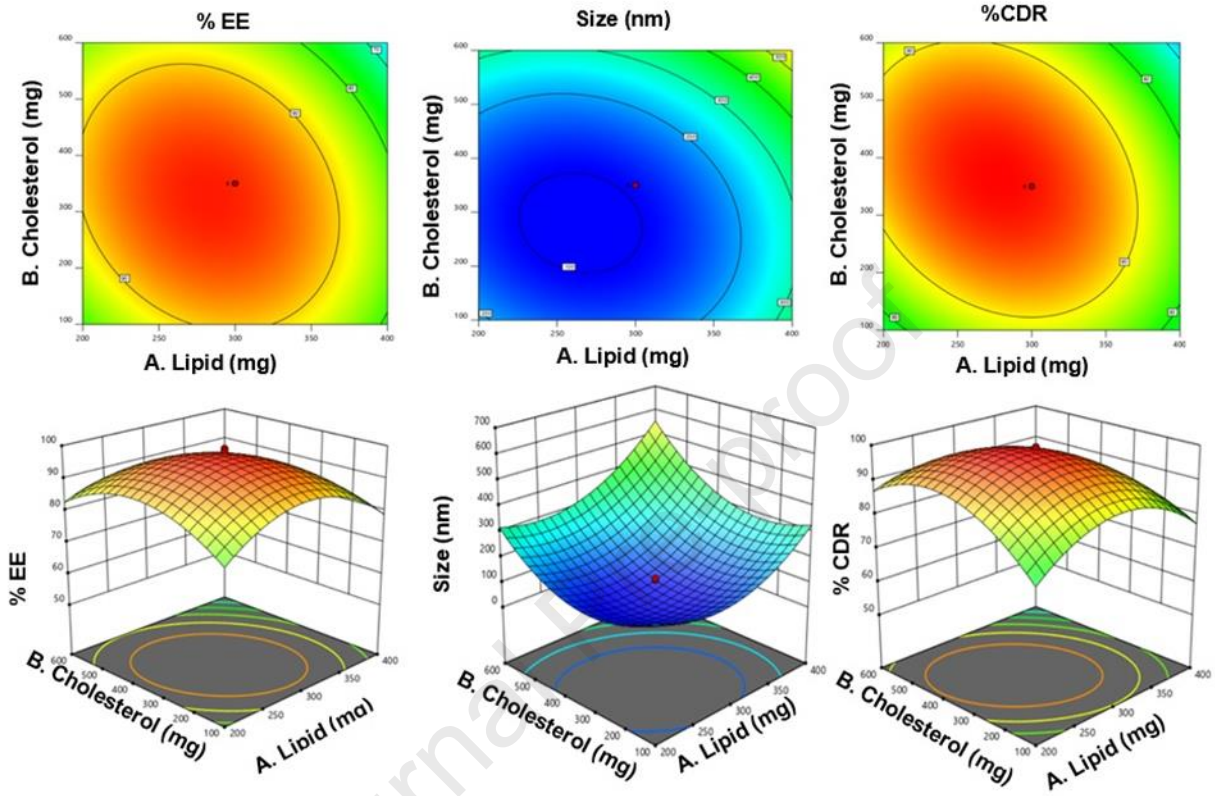

Figure 3. Counter plots and response surface plots (3D) showing the interactive effects (i) amount of lipid and (ii) amount of span 60 on % EE Y1, (A & B) on vesicle size Y2, (C & D) and % CDR (E & F).

Validation of the developed model and selection of optimized formulation

We use correlation plots between observed and anticipated values to create polynomial quadratic models. As demonstrated in Figure 4, there is a statistically significant connection between a model's anticipated value and a response's actual value.

For the responses Y1, Y2, and Y3, R2 values of 0.9806, 0.9834, and 0.9864 were obtained. The study's significant R2 values proved the proposed model's validity. To pick the best liposomal formulation, we used the point prediction technique of the program to select the twenty trial formulations made according to the CCD. A complete examination found that the loaded liposomes

F12 (300mg of Cholesterol, 350mg of Soya Lecithin, and 1.5ml of Span 60) matched all the criteria for an optimum formulation.

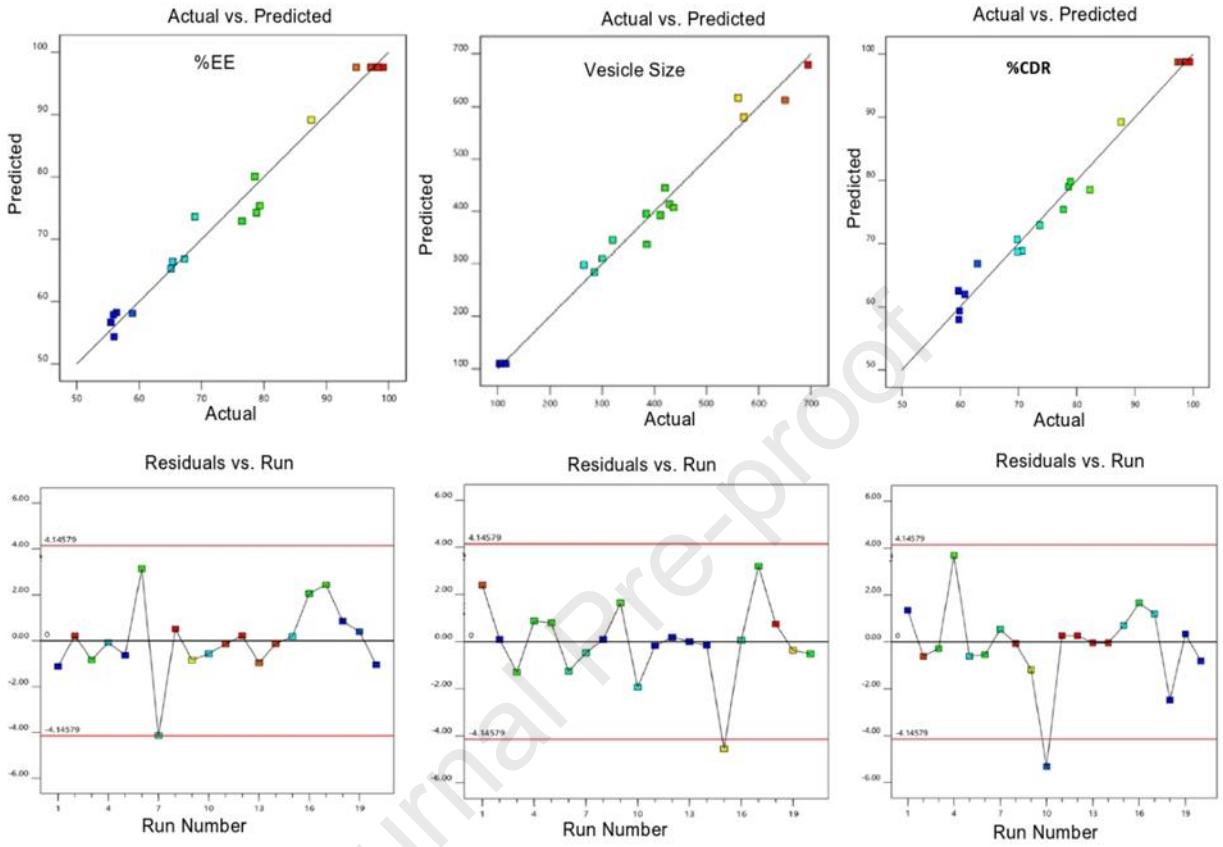

Figure 4. Actual and Predicted Values of % EE, % CDR, Particle Size.

Table 4. ANOVA for Quadratic model**.**

Parameter	source	DF	Sum of squares	Mean of squares	F Value	*P*-Value
%EE	Model	9	8082.72	564.75	56.14	< 0.0001
	Residual	10	100.60	10.60		
	Lack of fit	5	89.22	17.84	7.84	0.0206
	Pure error	5	15.55	3.11		
SIZE	Model	9	6.747E+05	74965.13	69.54	< 0.0001
	Residual	10	11368.43	1136.84		
	Lack of fit	5	11258.52	2251.70	102.43	< 0.0001

	Pure error	5	109.91	21.98		
%CDR	Model	9	4313.44	479.27	80.62	< 0.0001
	Residual	10	59.45	5.94		
	Lack of fit	5	56.69	11.34	20.56	0.0024
	Pure error	5	2.76	0.5514		

Evaluation of Liposomes

The optimized liposomal formulation (F12) showed 98.26±1.06 % EE, 103.82±7.16 nm Vesicle size, and % CDR is 99.38±0.16, -10mV to -32.8 zeta potential, and 0.251 PDI with spherical morphology [17].

The negative zeta potential values indicate that the dispersed particles in the suspension indicated a colloidal suspension leading to a negative charge. Also, there is a possibility of orientation of oxygen atom in its structure, giving rise to a negative potential. The zeta potential represents the aqueous system's micelle surface charge. Nanomicelles with a higher zeta potential has more interparticle repulsion, which improves system stability. Due to the high repulsive forces between them, the particles will not coagulate and remain suspended. The Zeta potentials of the blank and ZMT liposomes were -10 mV and -32.8 mV, respectively. The addition of ZMT into the micelles may have caused a change in the zeta potential of ZMT liposomes. A higher zeta potential value indicated that the ZMT liposomal suspension had good stability characteristics.

The percentage of EE, CDR, and the vesicle size was inversely related to the amount of soya lecithin in the formulation and directly proportional to the amounts of ethanol and Cholesterol. A higher percentage of EE is soon attained when liposomes are dispersed in lipid. Soya lecithin readily dissolves ZMT, a lipophilic drug, indicating that raising the concentration of soya lecithin is the most crucial element in increasing the percent EE. For the first time, it has been shown that lipophilic medicines may be effectively solubilized with the aid of alcohol. The hydrophobicity and solvent capacity of ZMT is excellent. Because of its polarity and partition coefficient, propylene glycol was included in the formula. Drugs delivered to the nasal mucosa benefit from their humectant and penetration-enhancing properties. F12's PDI and zeta potential

indicate that the liposomal formulation is stable. The zeta potential plays a significant role in colloidal dispersion stability [18,19].

The liposome vesicles' morphology was investigated using scanning and transmission electron microscopy (SEM and TEM). SEM revealed the smooth and spherical structure of ZMT liposomal vesicles. The TEM studies showed that the morphological characteristics of optimized LGF are uniformly distributed [20].

Determination of gelation temperature

We found that the optimized gelation temperature of Poloxamer-188 was 30-34o C, i.e., the nasal cavity temperature. At a concentration of 14 % w/v. Poloxamer-188 has thermo reversibility, which is responsible for the negative solubility coefficient and inhibits copolymer micelles. It is an aqueous copolymer of propylene and ethylene oxide in low concentrations and forms micelles and multimolecular aggregates, whereas it forms a gel at higher concentrations [17] (Table 5). It was shown that gels having a sol-gel transition temperature of 30 to 34°C react with the nasal mucosa to create gelations in situ. Various combinations of mucoadhesive polymers were examined in the test samples (Table 6).

Table 5. Results of gelation temperature.

S.No.	Poloxamer 188 (%w/v)	Gelation temperature (^{0}C)
1	10	No gelling till 42
2	11	No gelling till 42
3	12	27-31
4	13	25-30
5	14	31-33
6	15	24-28
7	16	Viscosity increased at 40

Table 6. Effect of mucoadhesive agents on gelation temperature of the formulation.

S.No	Formulation	Poloxamer 188	Carbopol 934	HPMV K100	Gelation temperature
1	G1	14	0.5	-	33.9±0.21
2	G2	14	1.0	-	33.7±0.43
3	G3	14	1.5	-	31.9±0.13
4	G4	14	-	0.5	34.2±0.26
5	G5	14	-	1.0	30.09±1.00
6	G6	14	-	1.5	28.9±2.30
7	G7	14	1.0	1.0	35.6±3.21

Poloxamer-188 and hydrogels have improvised the intranasal drug administration because of their mucoadhesive nature. They could open the stretched junctions and intern reversibly enhance the drug absorption and permeation [21]. The gelation mechanisms involve interactive forces, such as electrostatic forces and increased hydrogen bonding between the polymer chains. Each formulation had a gelation temperature ranging from 28.9 2.30 to 35.6 3.21o C, which is excellent for nasal gel formulations. Due to HPMC-K100 (G1quick's) effective gelling process, we discovered that the gelation temperature in the absence of this polymer was high. It might be because the use of 1.5 percent w/v HPMC-K100 (G6) increased the gelation.

In-situ ZMT liposomal nasal gel formulation and its evaluation

With Poloxamer-188 and mucoadhesive agents, the ZMT-LGF formulation was improved in situ (0.5-1.5 percent of both Carbopol-934 and HPMC-K100). Mucoadhesive agents were adjusted based on their impact on the viscosity, gel strength, gelation temperature, and the mucoadhesive strength of the mixture. It was determined that gel strength was the most crucial factor in formulating G3 and G6, which had a gelation temperature of 30 to 32 oC and high mucoadhesive strength, respectively. Formulas with gel strengths more significant than in the 1950s are stiff and irritating to patients [22]. Formulations with gelation temperatures over 35 oC

risk drug loss regarding handling and use. Gelation temperatures lower than 25 °C may cause stability issues.

Nasal mucosa has a pH range of 4.5 to 6.5 and can handle a pH range of 3 to 10. The improved gel's pH was 5.8 0.5, which is comfortable and appropriate for nasal research. The liposomal gel's drug content ranged from 98 to 99 percent, while the liposomal gel's mucoadhesive strength and viscosity were directly proportional to the quantities in the liposomal gel. Carbopol-934 is a carboxylic group-containing polyacrylate polymer that forms hydrogen bonds with the mucosal surface of the nasal cavity, boosting mucoadhesive strength. The hydrophilicity of HPMC increases the gel strength resulting in the formation of a rigid gel. HPMC undergoes rapid hydration after exposure to an aqueous environment, resulting in chain relaxation and increased viscous gelation [23]. Due to greater mucoadhesive strength and gel formation, drug retention in the nasal cavity is prolonged, thus enhancing its permeability.

Fourier Transform Infrared Spectroscopy (FT-IR) Studies

FT-IR spectroscopy of treated skin vesicles was used to investigate the influence of vesicle therapy on the biomechanics of skin lipids organization. Using phosphate buffer saline (pH 7.3) as a reference, we measured the FT-IR spectra of skin exposed to various solutions, including excipients, drugs, and tailored liposomes. An FT-IR examination reveals the skin's biophysical condition by examining the molecular conformational changes of fatty acyl chains of proteins and lipids. Skin lipid hydrocarbon chains were found to have asymmetric and symmetric C-H vibration peaks at 2950 and 2850 cm1 in rat FT-IR spectra. The lipid disruption and extraction of skin lipids can be seen in these two peaks' height, size, and displacement. This peak region is significantly broadened in the elastic liposomal formulation-treated skin, demonstrating its lipid perturbation action. It was reported that a decrease in the area of this peak indicated lipid extraction. In contrast, a broadening and diseaperind of this peak showed the vehicle's lipid disruption activity on the skin surface. The elastic liposomal formulation-treated skin's broadening of the peak is primarily due to soya lecithin and Cholesterol, which have been documented to have lipid disruption effects on skin lipid **(Figure 5).**

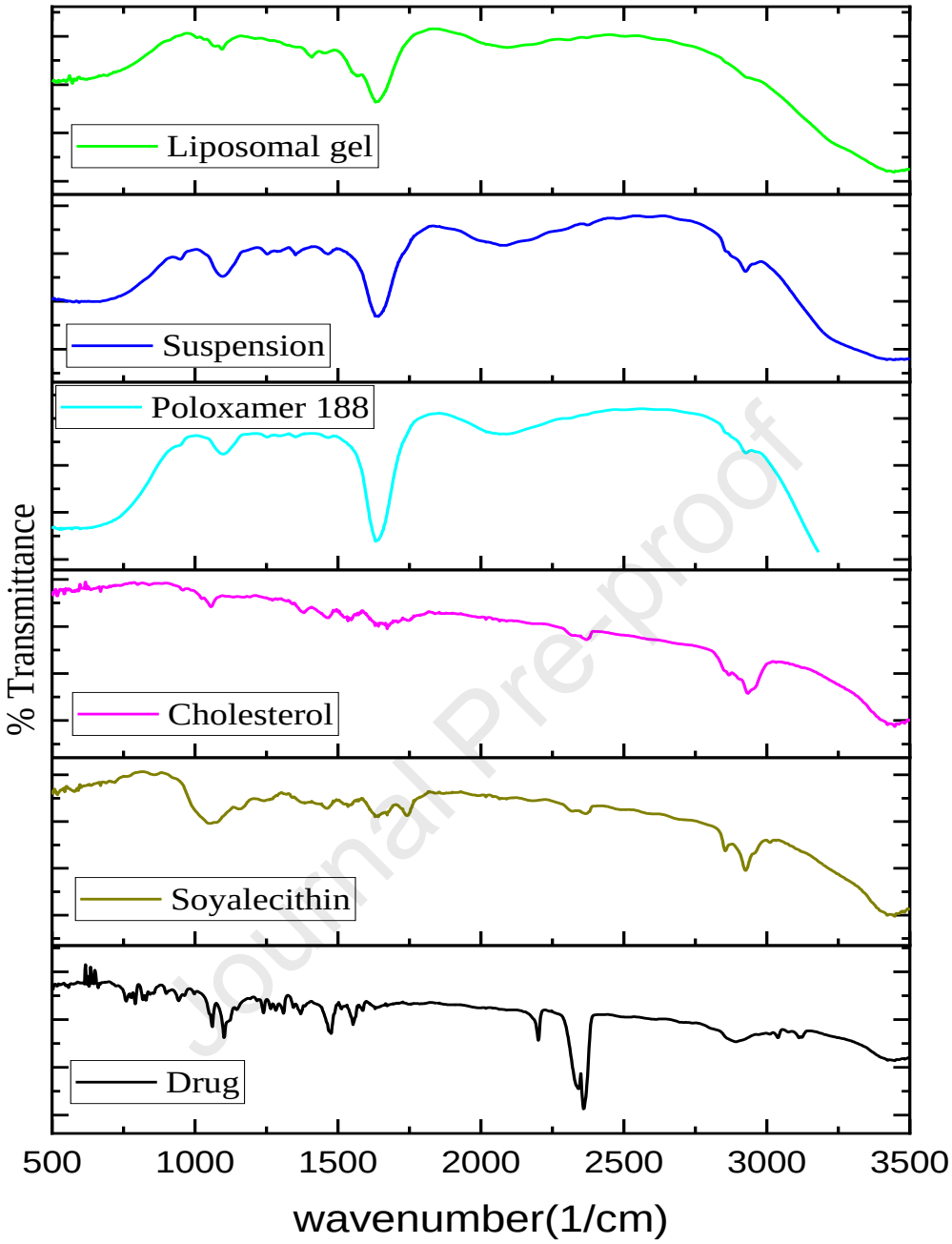

Figure 5. Drug compatibility studies FT-IR spectral data of a. ZMT API, b. Soya lecithin, c. Cholesterol, d. Poloxamer188 e. Liposomal suspension, and f. Liposomal gel.

Differential Scanning Calorimetry (DSC)

ZMT liposome DSC thermograms are shown in Figure 6. 136.50 was the endothermic peak of the substance, according to the data. It has a crystallized appearance. Whereas the suspension and gel peaks were observed at 199.18 and 249.97, respectively, indicating the amorphic nature of

the formulation. The temperature of the Liposomal suspension peaked at 199.18 °C on the thermogram. However, there was no such peak on the thermogram of the ZMT liposome, indicating that the drug was equally diffused at the molecular level (i.e., amorphous) in the bilayer. The disappearance of sharp peaks showed a considerable reduction in drug crystallinity. The medication and other excipients have no substantial chemical interactions.

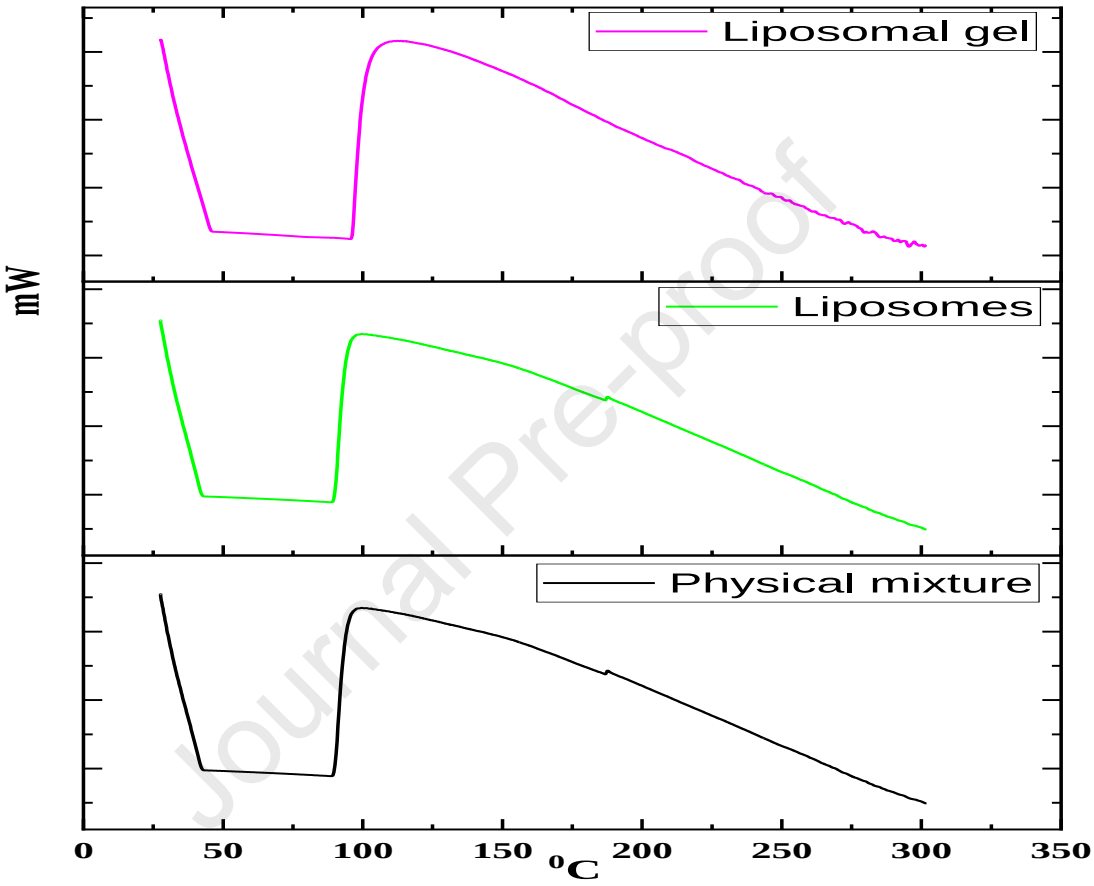

Figure 6. Drug compatibility studies DSC spectral data of a. Pure Drug. b. Liposomal suspension and c. Liposomal gel

X-ray diffraction (XRD)

Figure. 7 exhibits the enlargement of diffraction peaks due to disordered states of crystals. This is because of the absence of interferences of X-rays in the lattice. The XRD pattern for ZMT liposomes was recorded over a 2θ range of 0 to 80°C. Sharp characteristic peaks appeared at 2θ = 12° and 38°C, exhibiting a polymorphic nature, vital for enhanced drug delivery performance.

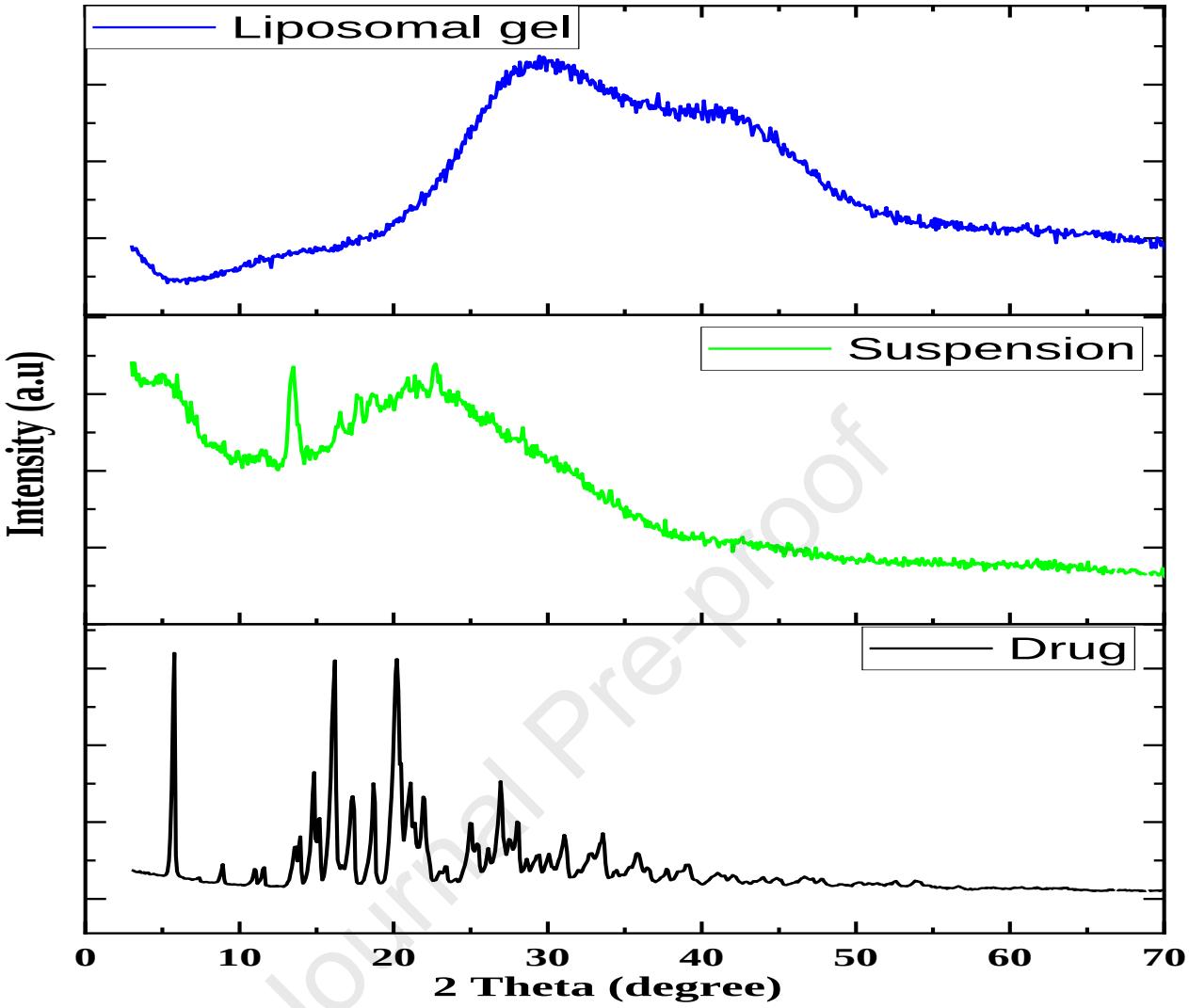

Figure 7. Drug compatibility studies XRD spectral data of a. Liposomal suspension, b. Liposomal gel.

Scanning Electron Microscopy (SEM), also known as TEM (SEM & TEM)

A TEM image of liposomal gel and suspension (Figure 8) shows the surface appearance and form under scanning electron microscopy (SEM). Each improved liposome formulation featured spherical-shaped particles, according to SEM examination. It was shown that the morphological properties of optimized LGF were evenly distributed in TEM examinations.

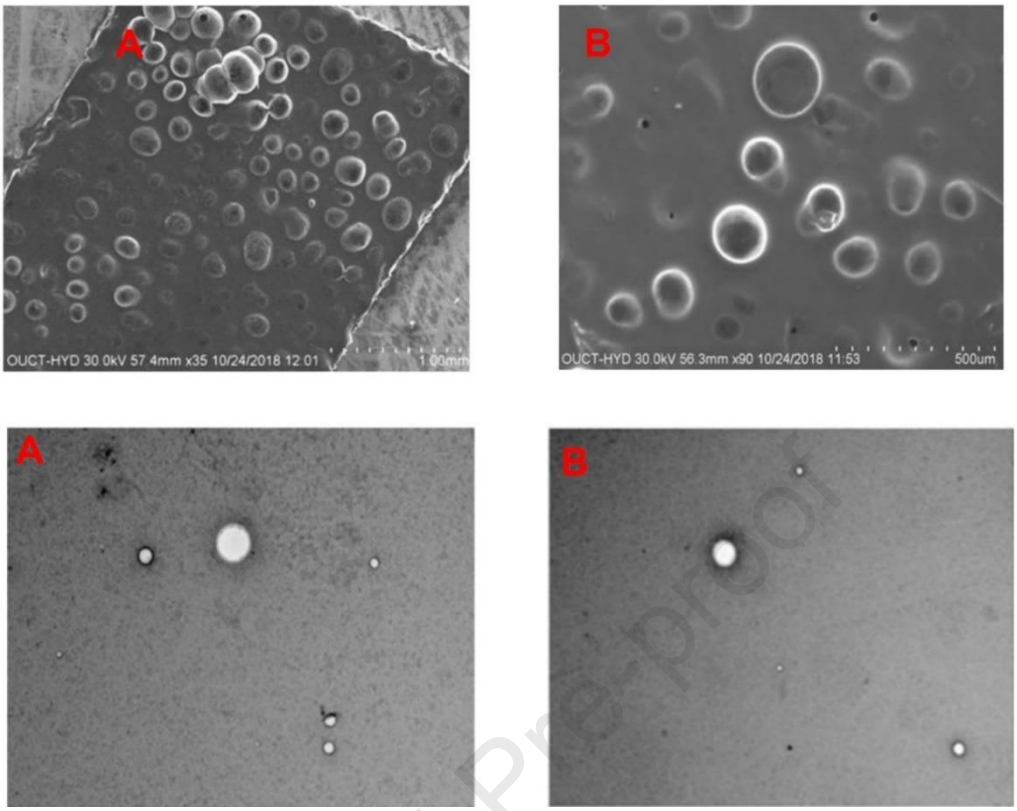

Figure 8. Morphological studies of Liposomal suspension and Liposomal gel by SEM (A) and TEM (B).

In Vitro % CDR of ZMT-Liposomal Intranasal Gel

Figure. 9 shows the In-vitro % CDR from ZMT optimized liposomal suspension and gel, hydrogels, and the composite formulation. An extended-release of ZMT- LGF was observed at 36 hours with an extended release of 90 % of CDR. We noticed that the optimized suspension showed 98 % of the drug release within 14 hours. Hydrogel (Carbopol-934) and composite formulations showed a release rate of 100% within 28 to 30 hours. Thus, drug diffuses according to different release kinetics when composition of the galenic form is modulated and/or liposomes are used. CDR experiments on G3 and G6 formulations comprising Carbopol-934 and HPMC-K100 showed no significant change after 24 hours, as indicated in Table 7. While Carbopol-934 was shown to be responsible for the release of the drug in G3, it was found to be responsible for the release of the drug in G6 [24].

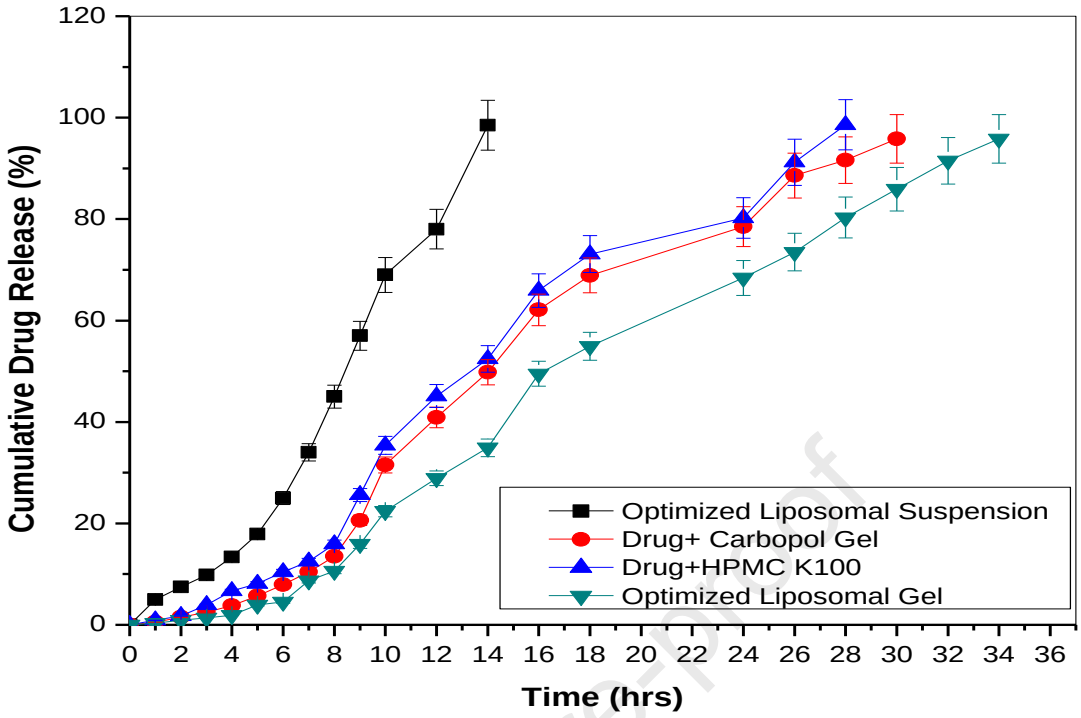

Figure 9. Drug release experiments in vitro utilizing formulations on Franz diffusion cells. All findings are expressed using the mean std. dev. (n = 3)

Table 7. Model fitting for optimized LGF (G3 and G6).

Formulation code models	Pure drug		Drug +poloxamer 188		G3		G6	
	Parameters	R2	Parameters	R2	Parameters	R2	Parameters	R2
Zero *(K0)*	15.12	0.79	10.012	0.95	6.59	0.72	6.02	0.98
First *(K1)*	0.79	0.97	0.19	0.92	0.13	0.99	0.106	0.99
Higuchi *(KH.)*	36.92	0.98	28.09	0.89	20.51	0.98	19.21	0.99
Korsemeyer-Peppas *(KKP)*	28.32 n=0.61	0.98	13.36 n=0.607	0.98	16.68 n=0.582	0.99	13.34 n=0.66	0.99
Hixson-Crow	0.098	0.99	0.05	0.99	0.035	0.98	0.029	0.99

Ex-vivo Permeation of ZMT-Liposomal Intranasal Gel

Figure 10 results of an ex-vivo permeation investigation employing Franz diffusion cells and freshly excised goat nasal mucosa as diffusion membrane in the Franz diffusion cells. For 18 hours, the ZMT was delivered in a sustained and regulated manner in the control gel formulation, highlighting the critical importance of the Optimized liposomal suspension and Gel. It was found that the findings of ex-vivo permeation research matched those of in-vitro drug release tests.

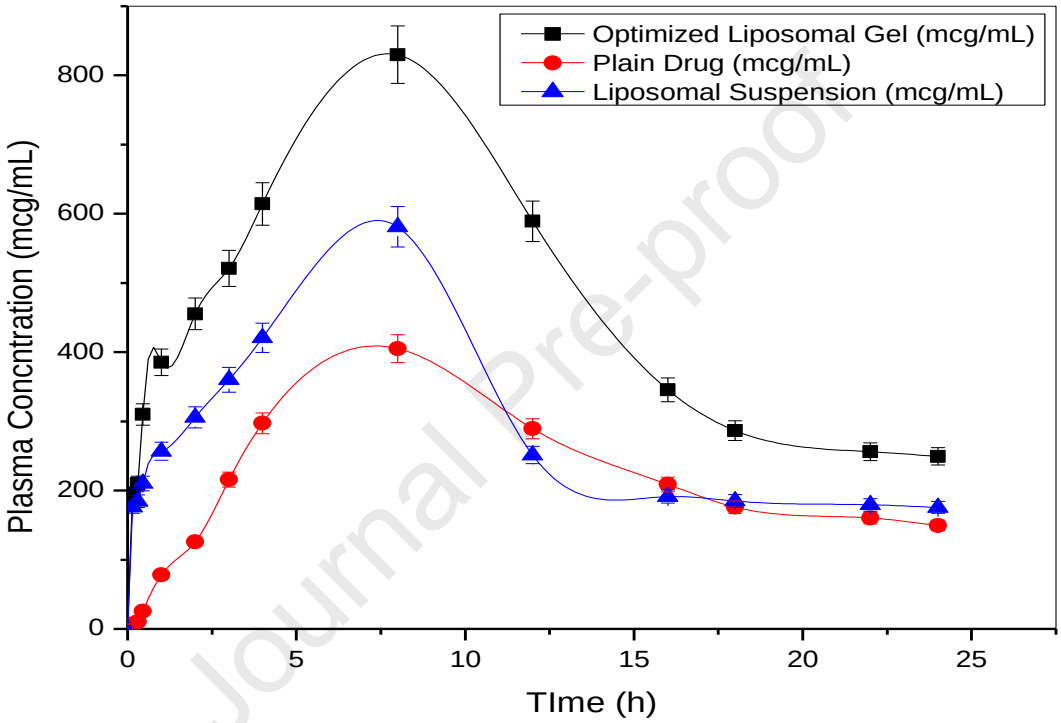

Figure 10. Testing formulations via freshly removed goat nasal mucosa for ex-vivo permeation studies.

Skin Irritation test

To examine the possible irritating effects of the developed ZMT liposomal formulation, rat skin irritation studies were carried out. A common irritant was a 0.5 percent v/v aqueous solution of para-formaldehyde. A little edema exfoliation was observed on the stratum corneum, and collagen dissociates due to the application of paraformaldehyde. Compared to the positive control group, the skin irritation test revealed no evidence of erythema or edema at the application site during the test time, indicating that the compositions were well tolerated by the skin. The ZMT lipid-based formulation was found to be safe for transdermal distribution.

Pharmacokinetics study of F12 and ZMT - loaded liposomal Gel

Six rabbits received an injection of the LGF, and the plasma concentrations are shown in Figure 11. Due to the smaller vesicle size of the Liposomal solution, F12 showed a greater drug plasma concentration as compared to ordinary ZMT-loaded Liposomal gel (F12). Activating the liposomal and liposomal suspensions in F12 with surfactant improves ZMT's absorption via the skin. Six rabbits' pharmacokinetic data are shown in **Table 8**. This is the medication's greatest (or peak) blood concentration that is attained in a particular test location following delivery. It is a standard measurement in the field of pharmacokinetics. F12 showed a significant Cmax compared to plain ZMT; it is approximately 10.7 times greater than ZMT. This was due to F12's higher bioavailability compared to plain ZMT and Liposomal suspension. The clearance (CL) and elimination rate constant (Ke) of both F12 and plain ZMT is significant ($p<0.05$). F12 and plain ZMT both had significant half-lives ($p<0.05$). The area represents the total drug exposure under the curve AUC (from zero to infinity). The AUC relates to the total amount of drugs absorbed by the body. This is useful for determining whether two formulations of the same dose deliver the same drug dose to the body; as a result, the area under the curve of F12 is significantly greater than that of plain ZMT and liposomal suspension. The greater the area under the curve of F12, the greater its bioavailability; it was approximately ten times greater than plain ZMT. The primary residence time of a drug molecule in the body is measured. As a result, F12, plain ZMT, and Liposomal Suspension had significantly different high residence times ($p<0.05$).

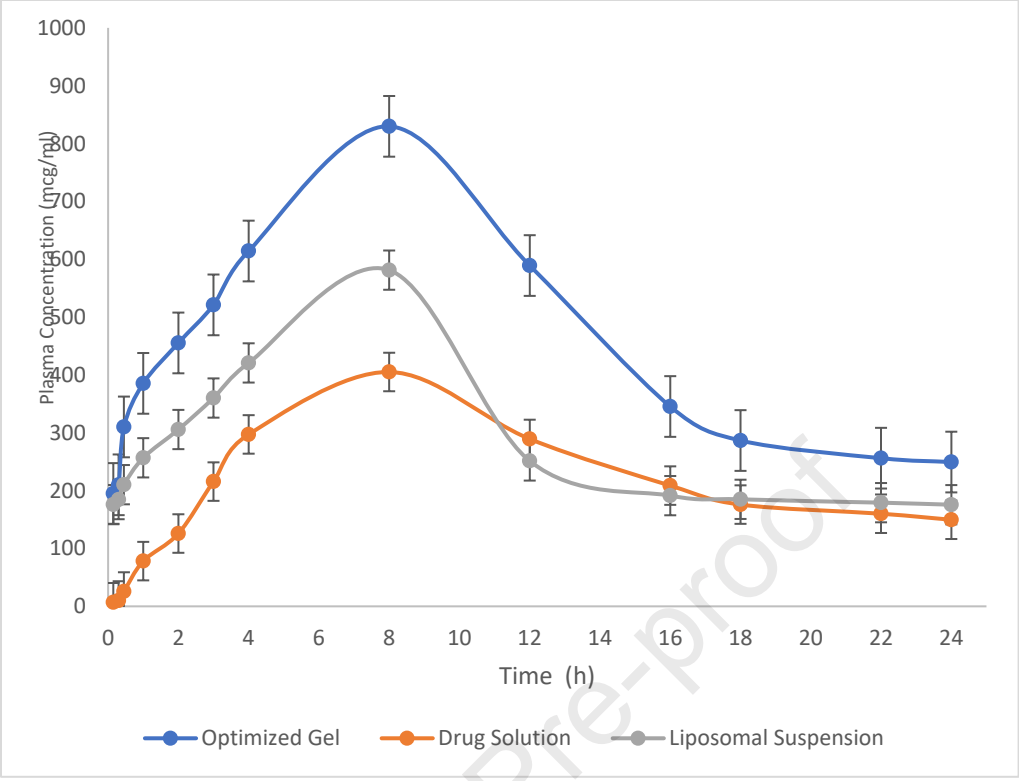

Figure 11. Plasma Concentration versus time profile of optimized liposomal gel, Drug solution, and Liposomal suspension.

Table 8. Pharmacokinetic parameters of optimized liposomal gel, Drug solution, and Liposomal suspension.

Pharmacokinetic Parameters	**Drug Solution**	**Liposomal Suspension**	**Optimized Gel**
Co mcg/mL	53.64	282.25	392.26
K hr-1	-0.07	0.015	0.007
Dose mg	2.5	2.5	2.5
Vd mL	46.60	8.86	6.373
$t_{1/2}$ hr	-9.28	45.26	89.65
Cl L/hr	-0.003	0.0001	0.00005
AUC-o-t mcg.hr/mL	1.21	6.353	8.829
AUC total- mcg.hr/mL	-465.52	13641.15	35563.78
C_{max}- mcg/mL/hr	398.12	581.2	829.77

T_{max}- ml/min	8	8	8

Histopathological evaluation

Results of histological experiments on the effects of hydrogel system on skin cell structure after application on the mucous membrane of Wistar Albino rats and the processes of drug permeability through the skin in Figure. 10. Histopathological examinations were performed on samples of skin, hydro-ethanolic way to solve skin, lipid nanoparticles suspension-treated skin, and LGF-treated skin [25]

Skin treated with normal saline signifies all five layers of skin (Figure. 12A). Optimized LGF-treated skin showed no signs of necrosis and inflammation (Figure. 12B). Mild thickening of hair follicles and damaged cells were observed on liposomal suspension treated skin (Figure. 12C), whereas skin treated with a hydroethanolic solution of the drug resulted in necrosis of cells, which inhibited the %CDR into the systemic circulation (Figure 12D). The optimized LGF was mucous-friendly and non-irritating and can be used in migraine therapy. The liposomal and nanoethosomal formulations of ZMT were shown to be more effective in delivering the medication via the nasal route, enhancing the bioavailability and duration of action.

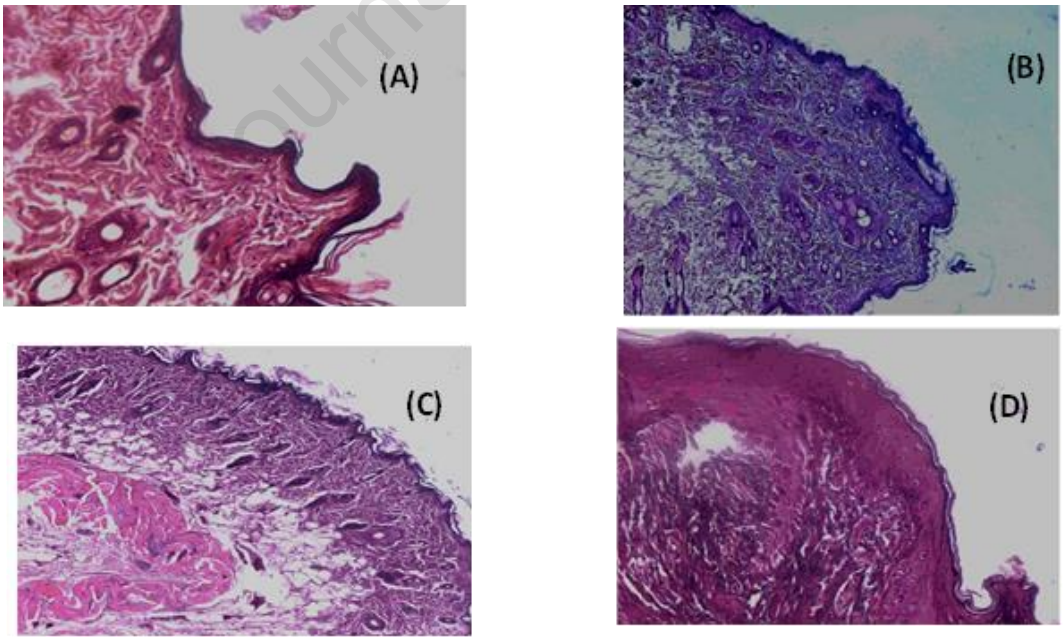

Figure 12. Histopathological evaluation of section of Wister albino rat mucosa. (A) Mucosal tissue treated with Normal Saline (B) Mucosal tissue treated with Liposomal Suspension (C) Mucosal tissue treated with Hydroalcoholic solution (D) Mucosal tissue treated with Liposomal gel.

Stability studies

The ZMT-liposomes were evaluated for their stability at diverse temperatures and pH values over 12 weeks. Liposomes stored at 25 to 40° C were found to be stable (Table 9).

Table 9. Results of stability studies of optimized formulation F-12 and G6.

Months	**Temperature**	**%EE**	**% CDR**	**Drug Content**	**Vesicle Size**	**Zeta value (mv)**
1st	(4±2ºc)	94.46±0.7	99.08±0.4	98.49±2.1	150.37±4.6	-34.4±1.64
2nd		92.34±2.1	96.45±0.1	98.12±1.1	167.42±3.8	-32.1±1.1
3rd		89.26±0.5	92.46±0.4	97.89±1.3	180.64±2.4	-30.9±1.4
1st	(30±2ºc)	94.46±0.7	99.08±0.4	98.49±2.1	150.37±4.6	-34.4±1.64
2nd		94.13±0.1	99.02±0.2	98.15±1.1	155.26±2.5	-33.1±0.38
3rd		93.46±0.4	98.19±0.1	97.89±0.3	160.45±1.4	-32.41±0.26
G6 -Formulation						
Months	Temperature	pH	Gelation Temperature	Size	Clearance	Drug Content
1st	(4±2ºc)	5.8	28.9±2.30	98.5±0.54	Very Smooth and Uniform	99.49±2.3
2nd		5.6	29.2±1.43	101.2±1.01		98.92±1.5
3rd		5.9	29.8±1,98	104.82±1.13		98.19±1.2
1st	(30±2ºc)	5.7	27.8±2.30	99.3±0.24	Very Smooth and Uniform	98.49±2.1
2nd		5.9	28.5±1.43	102.6±1.50		98.15±1.1
3rd		6.1	29.3±1,44	105.31±0.53		97.89±0.3

Note: No significant difference in the stability parameters assessed at varied temperatures indicates the stability of the optimized liposomal suspension and gel formulation.

ZMT affinity with Micelle (Soya Lecithin+Cholesterol)- Docking studies

The micelle has been designed using Cholesterol as a copolymer. ZMT entrapment has been studied with micelle, whether the drug will entrap in the polar head or not. The polar head of the micelle has a high binding affinity for the medication (kcal/mol). With the creation of four hydrogen bonds, ZMT showed a binding affinity of -2.7 kcal/mol (two conventional and two carbon-hydrogen). Table 10 displays the ZMT docked with micelle's ligand energy (kcal/mol), binding affinity (kcal/mol), and RMSD values. The micelle-binding positions of ZMT are shown in the **Figure 13.**

Table 10. The ligand energy (kcal/mol), binding affinity (kcal/mol), and rmsd values of ZMT docked with micelle.

Ligand Energy (kcal/mol)	Binding Affinity (kcal/mol)	rmsd/ub	rmsd/lb
584.01	-2.7	0	0
	-2.6	14.62	12.25
	-2.5	20.53	17.88
	-2.5	15.62	12.53
	-2.5	15.45	11.35
	-2.5	5.47	3.009
	-2.4	20.51	18.82
	-2.4	5.99	3.29
	-2.4	19.84	17.38

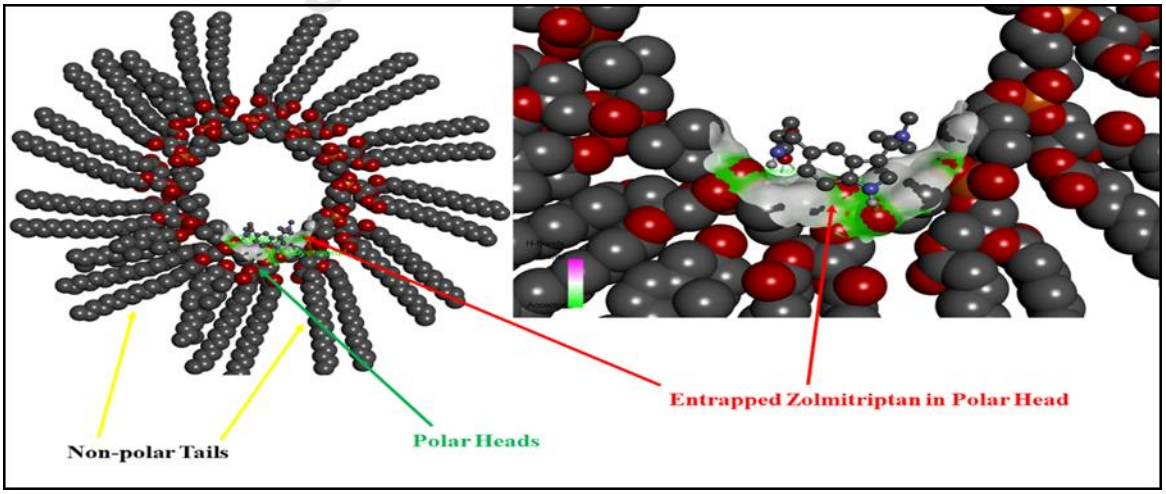

Figure 13. The binding poses of ZMT in the polar head of Soya Lecithin in the presence of Cholesterol

Conclusions

The CCD of the ZMT optimized formulation showed a correlation between independent and dependent variables. The optimized ZMT -loaded liposomal formulation F12 exhibited the maximum EE of 98.26±1.06%. EE also suggested that the optimal concentration required for % EE for the % CDR of 99.38 % is a moderate concentration of Cholesterol, soya lecithin, and span-60. The ZMT -loaded liposomal formulation using Poloxamer-188 and HPMC-K100, and Carbopol-934 exhibited Muco-adhesive agents with the thermos-reversible property of the polymer. The optimized gel formulations G3 and G6 positively correlated with gelation temperature, which showed relatively similar permeability and % CDR pattern. According to our molecular docking investigations, micelle-bound medication had binding energy of -2.7 kcal/mol, forming two conventional bonds and a carbon-hydrogen bond on two separate occasions. The micelle is stable since ZMT is perfectly entrapped in the polar head of the particle. Our in-silico experiments recommend developing ZMT's micellar drug delivery system to enhance medication delivery across the blood-brain barrier. There are no or minimal adverse effects from the newly developed ZMT-LGF, which has improved effectiveness, acceptable tolerability, and greater bioavailability, making it an ideal formulation for treating acute Migraines.

Credit authorship contribution statement: Conceptualization, Chetupalli A. K, Sunand Katta; Data curation, Mohd. Vaseem Fateh; Formal analysis, M. Akiful Haque; Investigation, Daniel Kothapally and M. Akiful Haque.; Methodology, Chetupalli A. K, Sunand Katta; Project administration, Mohd. Vaseem Fateh; Resources, Dr. Prasanth Damarasingu; Software, Chetupalli A. K; Visualization, Budumuru padmasri; Writing – original draft, Palavalasa Archana and Budumuru padmasri; Writing – review & editing, M. Akiful Haque and Mohd. Vaseem Fateh.

Declaration of competing interest: The authors declare no conflict of interest.

Supplementary Materials: Not applicable

Funding: This research received no external funding.

Data Availability Statement: Not applicable.

Acknowledgments: The Authors are thankful to Anurag University for their support to carry out this research.

Institutional Review Board Statement: The animal research was carried out by CPCSEA norms and with approval from the Institutional Animal Ethics Committee in Nalgonda, Telangana, India (Ref. No. I/IAEC/NCP/009/2020R).

References:

1. Goadsby, P.J.; Lipton, R.B.; Ferrari, M.D. Migraine—current understanding and treatment. N. Engl. J. Med. 2002, 346, 257–270.
2. Liu, C.; Fang, L. Drug in adhesive patch of ZMT: formulation and in vitro/in vivo correlation. AAPS PharmSciTech 2015, 16, 1245–1253.
3. Ravi, P.R.; Aditya, N.; Patil, S.; Cherian, L. Nasal in-situ gels for delivery of rasagiline mesylate: improvement in bioavailability and brain localization. Drug Deliv. 2015, 22, 903–910.
4. Altunta\cs, E.; Yener, G. Formulation and evaluation of thermoreversible in situ nasal gels containing mometasone furoate for allergic rhinitis. AAPS PharmSciTech 2017, 18, 2673–2682.
5. Zaki, N.M.; Awad, G.A.; Mortada, N.D.; Abd ElHady, S.S. Enhanced bioavailability of metoclopramide HCl by intranasal administration of a mucoadhesive in situ gel with modulated rheological and mucociliary transport properties. Eur. J. Pharm. Sci. 2007, 32, 296–307.
6. Lappenberg-Pelzer, M. Identification and determination of opipramol metabolites in plasma and urine. J. Anal. Toxicol. 1998, 22, 215–219, doi:10.1093/jat/22.3.215.
7. Shinde, G.; Desai, P.; Shelke, S.; Patel, R.; Bangale, G.; Kulkarni, D. Mometasone furoate-loaded aspasomal gel for topical treatment of psoriasis: formulation, optimization, in vitro and in vivo performance. J. Dermatolog. Treat. 2020, 1–12.
8. Marques, A.C.; Rocha, A.I.; Leal, P.; Estanqueiro, M.; Lobo, J.M.S. Development and characterization of mucoadhesive buccal gels containing lipid nanoparticles of ibuprofen. Int. J. Pharm. 2017, 533, 455–462.
9. Shelke, S.; Pathan, I.; Shinde, G.; Agrawal, G.; Damale, M.; Chouthe, R.; Panzade, P.; Kulkarni, D. Poloxamer-Based In Situ Nasal Gel of Naratriptan Hydrochloride Deformable Vesicles for Brain Targeting. Bionanoscience 2020, 10, 633–648.

10. Nasri, S.; Ebrahimi-Hosseinzadeh, B.; Rahaie, M.; Hatamian-Zarmi, A.; Sahraeian, R. Thymoquinone-loaded ethosome with breast cancer potential: optimization, in vitro and biological assessment. J. Nanostructure Chem. 2020, 10, 19–31.
11. Ganguly, S.; Dash, A.K. A novel in situ gel for sustained drug delivery and targeting. Int. J. Pharm. 2004, 276, 83–92.
12. Agrawal, G.; Wakte, P.; Shelke, S. Formulation optimization of human insulin loaded microspheres for controlled oral delivery using response surface methodology. Endocrine, Metab. Immune Disord. Targets (Formerly Curr. Drug Targets-Immune, Endocr. Metab. Disord. 2017, 17, 149–165.
13. Ibrahim, T.M.; Abdallah, M.H.; El-Megrab, N.A.; El-Nahas, H.M. Transdermal ethosomal gel nanocarriers; a promising strategy for enhancement of anti-hypertensive effect of carvedilol. J. Liposome Res. 2019, 29, 215–228.
14. Fathalla, D.; Youssef, E.M.K.; Soliman, G.M. Liposomal and ethosomal gels for the topical delivery of anthralin: preparation, comparative evaluation and clinical assessment in psoriatic patients. Pharmaceutics 2020, 12, 446.
15. Talluri, S.V.; Kuppusamy, G.; Karri, V.V.S.R.; Yamjala, K.; Wadhwani, A.; Madhunapantula, S. V; Pindiprolu, S.S.S. Application of quality-by-design approach to optimize diallyl disulfide-loaded solid lipid nanoparticles. Artif. Cells, Nanomedicine, Biotechnol. 2017, 45, 474–488.
16. Khan, S.; Patil, K.; Bobade, N.; Yeole, P.; Gaikwad, R. Formulation of intranasal mucoadhesive temperature-mediated in situ gel containing ropinirole and evaluation of brain targeting efficiency in rats. J. Drug Target. 2010, 18, 223–234.
17. Luppi, B.; Bigucci, F.; Cerchiara, T.; Zecchi, V. Chitosan-based hydrogels for nasal drug delivery: from inserts to nanoparticles. Expert Opin. Drug Deliv. 2010, 7, 811–828.
18. Zhou, H.Y.; Jiang, L.J.; Cao, P.P.; Li, J.B.; Chen, X.G. Glycerophosphate-based chitosan thermosensitive hydrogels and their biomedical applications. Carbohydr. Polym. 2015, 117, 524–536.
19. Sherafudeen, S.P.; Vasantha, P.V. Development and evaluation of in situ nasal gel formulations of loratadine. Res. Pharm. Sci. 2015, 10, 466.

20. Shariat, S.; Badiee, A.; Jaafari, M.R.; Mortazavi, S.A. Optimization of a method to prepare liposomes containing HER2/Neu-derived peptide as a vaccine delivery system for breast cancer. Iran. J. Pharm. Res. IJPR 2014, 13, 15.
21. Li, C.; Zhang, X.; Huang, X.; Wang, X.; Liao, G.; Chen, Z. Preparation and characterization of flexible nanoliposomes loaded with daptomycin, a novel antibiotic, for topical skin therapy. Int. J. Nanomedicine 2013, 8, 1285.
22. Verekar, R.R.; Gurav, S.S.; Bolmal, U. Thermosensitive mucoadhesive in situ gel for intranasal delivery of Almotriptan malate: Formulation, characterization, and evaluation. J. Drug Deliv. Sci. Technol. 2020, 58, 101778.
23. Alnasser, S. A review on nasal drug delivery system and its contribution in therapeutic management. Asian J. Pharm. Clin. Res. 2019, 12, 40–45.
24. Mamindla, P.; Mogilicherla, S.; Enumula, D.; Prasad, O.P.; Anchuri, S.S. A review on Migraine. Acta Sci. Pharm Sci 2019, 3, 29–42.
25. Ways, T.M.M.; Lau, W.M.; Khutoryanskiy, V. V Chitosan and its derivatives for application in mucoadhesive drug delivery systems. Polymers (Basel). 2018, 10, 267.
26. Sridhar, V.; Wairkar, S.; Gaud, R.; Bajaj, A.; Meshram, P. Brain targeted delivery of mucoadhesive thermosensitive nasal gel of selegiline hydrochloride for treatment of Parkinson's disease. J. Drug Target. 2018, 26, 150–161.
27. Lin, W.; Xie, X.; Yang, Y.; Fu, X.; Liu, H.; Yang, Y.; Deng, J. Thermosensitive magnetic liposomes with doxorubicin cell-penetrating peptides conjugate for enhanced and targeted cancer therapy. Drug Deliv. 2016, 23, 3436–3443.
28. Mahmood, S.; Mandal, U.K.; Chatterjee, B. Transdermal delivery of raloxifene HCl via ethosomal system: Formulation, advanced characterizations and pharmacokinetic evaluation. Int. J. Pharm. 2018, 542, 36–46.
29. Ismail, T.A.; Shehata, T.M.; Mohamed, D.I.; Elsewedy, H.S.; Soliman, W.E. Quality by design for development, optimization and characterization of brucine ethosomal gel for skin cancer delivery. Molecules 2021, 26, 3454.
30. Amarachinta, P.R.; Sharma, G.; Samed, N.; Chettupalli, A.K.; Alle, M.; Kim, J.-C. Central composite design for the development of carvedilol-loaded transdermal ethosomal hydrogel for extended and enhanced anti-hypertensive effect. J. Nanobiotechnology 2021, 19, 1–15.

31. reza Ariamoghaddam, A.; Ebrahimi-Hosseinzadeh, B.; Hatamian-Zarmi, A.; Sahraeian, R. In vivo anti-obesity efficacy of curcumin loaded nanofibers transdermal patches in high-fat diet induced obese rats. Mater. Sci. Eng. C 2018, 92, 161–171.
32. Woo, F.Y.; Basri, M.; Masoumi, H.R.F.; Ahmad, M.B.; Ismail, M. Formulation optimization of galantamine hydrobromide loaded gel drug reservoirs in transdermal patch for Alzheimer's disease. Int. J. Nanomedicine 2015, 10, 3879.
33. Abdel Messih, H.A.; Ishak, R.A.H.; Geneidi, A.S.; Mansour, S. Nanoethosomes for transdermal delivery of tropisetron HCl: multi-factorial predictive modeling, characterization, and ex vivo skin permeation. Drug Dev. Ind. Pharm. 2017, 43, 958–971.
34. Pathan, I.B.; Jaware, B.P.; Shelke, S.; Ambekar, W. Curcumin loaded ethosomes for transdermal application: Formulation, optimization, in-vitro and in-vivo study. J. Drug Deliv. Sci. Technol. 2018, 44, 49–57.
35. Li, Y.; Xu, F.; Li, X.; Chen, S.-Y.; Huang, L.-Y.; Bian, Y.-Y.; Wang, J.; Shu, Y.-T.; Yan, G.-J.; Dong, J.; et al. Development of curcumin-loaded composite phospholipid ethosomes for enhanced skin permeability and vesicle stability. Int. J. Pharm. 2021, 592, 119936.
36. Chen, X.; Zhu, L.; Li, R.; Pang, L.; Zhu, S.; Ma, J.; Du, L.; Jin, Y. Electroporation-enhanced transdermal drug delivery: Effects of logP, pKa, solubility and penetration time. Eur. J. Pharm. Sci. 2020, 151, 105410.
37. Madhavi, N.; Sudhakar, B.; Reddy, K.V.N.S.; Ratna, J.V. Design by optimization and comparative evaluation of vesicular gels of etodolac for transdermal delivery. Drug Dev. Ind. Pharm. 2019, 45, 611–628.
38. Sakdiset, P.; Amnuaikit, T.; Pichayakorn, W.; Pinsuwan, S. Formulation development of ethosomes containing indomethacin for transdermal delivery. J. Drug Deliv. Sci. Technol. 2019, 52, 760–768.
39. Azeem, A.; Ahmad, F.J.; Khar, R.K.; Talegaonkar, S. Nanocarrier for the transdermal delivery of an antiparkinsonian drug. AAPS PharmSciTech 2009, 10, 1093–1103.
40. Kapoor, M.S.; D'Souza, A.; Aibani, N.; Nair, S.S.; Sandbhor, P.; Banerjee, R.; others Stable Liposome in Cosmetic Platforms for Transdermal Folic acid delivery for fortification and treatment of micronutrient deficiencies. Sci. Rep. 2018, 8, 1–12.

41. Jain, S.; Patel, N.; Madan, P.; Lin, S. Quality by design approach for formulation, evaluation and statistical optimization of diclofenac-loaded ethosomes via transdermal route. Pharm. Dev. Technol. 2015, 20, 473–489.
42. Dallakyan, S.; Olson, A.J. Small-molecule library screening by docking with PyRx. Chem. Biol. 2015, 243–250.
43. Rappé, A.K.; Casewit, C.J.; Colwell, K.S.; Goddard, W.A.; Skiff, W.M. UFF, a Full Periodic Table Force Field for Molecular Mechanics and Molecular Dynamics Simulations. J. Am. Chem. Soc. 1992, 114, 10024–10035, doi:10.1021/ja00051a040.
44. Khan, S.L.; Siddiqui, F.A.; Jain, S.P.; Sonwane, G.M. Discovery of potential inhibitors of SARS-CoV-2 (COVID-19) main protease (Mpro) from Nigella Sativa (Black Seed) by molecular docking study. Coronaviruses 2021, 2, 384–402.

Acknowledgment:

The Authors are thankful to Anurag University for their support to carry out this research.

Data Availability Statement:

Not applicable.

Declaration of competing interest:

The authors declare no conflict of interest.